Low-threshold spatial solitons in reverse-proton-exchanged periodically poled lithium niobate waveguides

Giuseppe Leo, Antonio Amoroso, Lorenzo Colace, and Gaetano Assanto

Nonlinear Optics and OptoElectronics Laboratory, National Institute for the Physics of Matter, Università "Roma Tre," Via della Vasca Navale 84, 00146 Rome, Italy

Rostislav V. Roussev and Martin M. Fejer

Edward L. Ginzton Laboratory, Stanford University, Stanford, California 94305-4085

Received March 3, 2004

Combining reverse proton exchange and uniform periodic poling in $LiNbO_3$ planar waveguides, we demonstrate low-energy spatial optical solitons by second-harmonic generation at room temperature, with a threshold as low as 23 pJ/μm at 1.5 μm. © 2004 Optical Society of America

OCIS codes: 190.0190, 190.5530, 190.4420.

Among the various techniques investigated for the fabrication of optical waveguides in $LiNbO_3$, Ti indiffusion and annealed proton exchange are the most successful. The latter requires a bath in a benzoic acid solution at moderate temperatures (≈200 °C; Ref. 1) and is often preferred in integrated optics because of the possibility of achieving stronger confinement of the optical fields.

Approximately a decade ago, reverse proton exchange (RPE) was introduced as a means to fabricate buried extraordinary-index $LiNbO_3$ waveguides.[2,3] In RPE, the proton-exchanged $LiNbO_3$ crystal undergoes a subsequent immersion in a Li-rich melt, which restores the Li^+ content (which had previously been replaced by H^+ ions at the exposed interfaces) and the $LiNbO_3$ refractive index at the surface. RPE buried waveguides allow for improved coupling from and to optical fibers owing to more-symmetric mode profiles and exhibit better confinement, increased overlap of pump and harmonic modal fields, and low scattering losses.[4]

In quadratic nonlinear optics, in addition to novel TE–TM nonlinear coupling,[5,6] RPE waveguides in z-cut $LiNbO_3$ are of interest because of their increased nonlinear conversion efficiency by means of an improved overlap integral between fundamental-frequency (FF) and second-harmonic (SH) TM modes and the reduced effect of the proton-exchanged layer's nonlinearity suppression. Recently, a combination of RPE and periodic poling was proposed for exploiting the above advantages within a quasi-phase-matching scheme,[7] and RPE buried channels fabricated in periodically poled $LiNbO_3$ (PPLN) have resulted in the highest second-harmonic generation (SHG) efficiency reported to date.[8] RPE PPLN planar waveguides are therefore natural candidates for $\chi^{(2)}$ one-dimensional spatial optical solitons, i.e., self-confined optical eigenwaves stemming from the balance of self-focusing and linear diffraction in the waveguide plane. Such solitons, or simultons, as they involve two frequencies with mutually locked phase velocities,[9] were previously demonstrated in Ti:indiffused $LiNbO_3$ waveguides that employed either nonuniform, noncritical phase matching along the propagation length[10] or quasi-phase matching[11] as well as in coupled RPE $LiNbO_3$ waveguides with TE–TM mode matching.[12] In this Letter we report, for the first time to our knowledge, low-threshold generation of one-dimensional spatial optical solitons in RPE PPLN planar waveguides.

$LiNbO_3$ wafers were periodically poled with quasi-phase-matched period Λ in poling stripes of width Γ normal to the propagation direction; several samples with different lengths L were diced out (see also Ref. 8). A sample with $\Lambda = 14.75$ μm, $\Gamma = 0.37$ mm, and $L = 2.75$ cm was proton exchanged for 24 h at 170.5 °C in benzoic acid to a depth of 1.2 μm and then annealed in air for 22.5 h at 312 °C. Subsequent reverse exchange involved immersion in a $LiNO_3$:KNO_3:$NaNO_3$ melt at 300 °C (Ref. 2) for 27 h in a ceramic beaker inside a tube furnace. Such a combination of proton exchange, annealing, and reverse exchange reduced the peak proton concentration after RPE to approximately one fifth of the as-exchanged level.

The experimental setup included an optical parametric oscillator plus optical parametric amplifier synchronously pumped by a frequency-doubled mode-locked Nd:YAG operating at 10 Hz with 25-ps pulses of a few hundred microjoules, tunable from 1100 to 1700 nm with a linewidth of <2 cm^{-1}. The specific time duration and spectral width prevented significant temporal walk-off and spectral filtering effects, respectively. After conditioning, a linearly polarized beam with a nearly Gaussian profile ($M^2 = 1.06$) was focused by a cylindrical telescope into an ellipitcal spot with a waist $w_z = 2.3$ μm deep and $w_y = 20$–70 μm in the waveguide plane; (see Fig. 1, inset). Such input was end-fire coupled in the waveguide with a 20× microscope objective. The sample was placed on a thermistor-controlled Peltier holder and kept at room temperature to prevent a nonuniform temperature (and hence phase-mismatch) distribution along the propagation length. Outputs at the FF and the SH were detected by photodiodes and (or) imaged onto a

0146-9592/04/151778-03$15.00/0

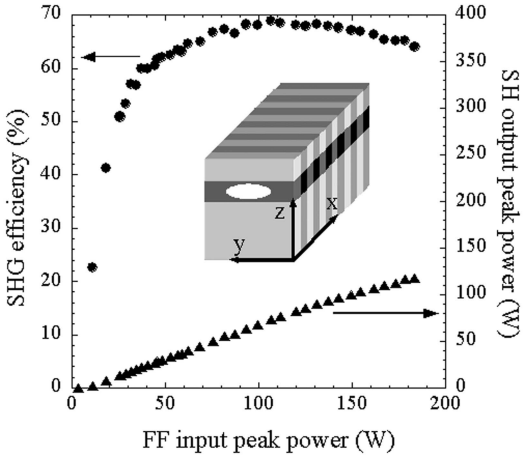

Fig. 1. SHG conversion efficiency (circles) and SH output (triangles) versus FF input at $\Delta\beta = 0$, with $w_y = 40$ μm. Inset, geometry of the sample and its excitation.

vidicon. Synchronous detection and real-time pulse filtering were implemented to reduce pulse-power fluctuations, and averaging helped to reduce the noise.

Exciting the TM_0 mode at FF (by use of a diode laser), we evaluated linear losses to be $\approx$0.78 dB/cm. Then, using the tunable source, we measured the SHG conversion efficiency versus wavelength to single out the phase-matching conditions and validate our waveguide modeling. Finally, we investigated soliton generation by systematically varying the FF peak power P, the wavelength, and the input waist.

The low-power SHG phase-matching wavelength and bandwidth (FWHM) were 1467.1 and 0.8 nm, respectively. The latter exceeds the value of 0.32 nm calculated in the cw limit because of the finite linewidth of the pump (0.22 nm at phase matching). Figure 1 shows the depletion curve for $w_y = 40$ μm, where the maximum SHG conversion efficiency is 69% at $P_{\mathrm{FF}} = 107$ W. Such efficiency is representative of all the quasi-phase-matched regions that we examined and is in agreement with numerical simulations, provided that the measured loss coefficients and an effective nonlinearity $d_{\mathrm{eff}} = K d_{\mathrm{eff,ideal}}$ are employed, where $K = 0.8$–1.0 and $d_{\mathrm{eff,ideal}} = 2d_{33}/\pi$, with $d_{33} = 27$ pm/V.

Soliton generation was investigated in terms of the variation of FF output spot size versus FF excitation and phase mismatch $\Delta\beta$, with $[\partial(\Delta\beta L)/\partial\lambda]_{\lambda\mathrm{pm}} \approx 5\pi/\mathrm{nm}$. Typical near-field FF output spots are displayed in Fig. 2: The beam narrowing at high FF power is obvious in comparison with the width of 158 μm in the linearly diffracted regime. Using a Gaussian fit, we graphed the narrowing in Fig. 3 for various phase mismatches and $w_y = 40$ μm (this makes $L = 3.8L_R$, where L_R is the Rayleigh range).

The minimum soliton threshold $P_{\mathrm{th}} = 140$ W (the power necessary to get an output spot size equal to the input) was obtained for a mismatch $\Delta\beta L = 2\pi$. Negative $\Delta\beta$ made P_{th} increase rapidly, whereas a less steep increase was observed for large positive values, in agreement with the predicted behavior.[13] This asymmetry with respect to $\Delta\beta L$ is visible in Fig. 4, where we plot the FF output spot size versus mismatch at constant excitation. For $\Delta\beta L < 0$, as the solitary SH component is expected to be larger, the monochromatic FF input eventually fails to generate a simulton. Because the threshold is related to the interplay between FF intensity and diffraction, we also acquired FF output spots for various input waists. For each w_y we determined P_{th} at an optimal mismatch (which always appeared within $\Delta\beta L/\pi = 2 \pm 0.5$). The data (triangles) are shown in Fig. 5: the expected decrease of soliton threshold for larger input waists was verified, with self-focusing for waists of 70 μm at FF fluences as low as 23 pJ/μm (energy density per unit of beam width) and a peak power of 75 W. The overlap integral in our samples, $I = \int f_{\mathrm{SH}}^{\mathrm{TM}_0}(z)\, |f_{\mathrm{FF}}^{\mathrm{TM}_0}(z)|^2 \mathrm{d}z = 3.46 \times 10^6 \Omega^{3/2}\ \mathrm{m}^{-1/2}$, in fact, is substantially larger than in standard surface waveguides ($\approx 2.5 \times 10^6 \Omega^{3/2}\ \mathrm{m}^{-1/2}$). Although for

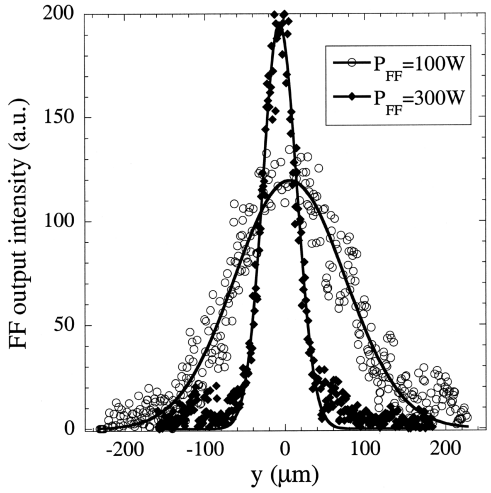

Fig. 2. FF output profiles at low (open circles) and high (squares) input power.

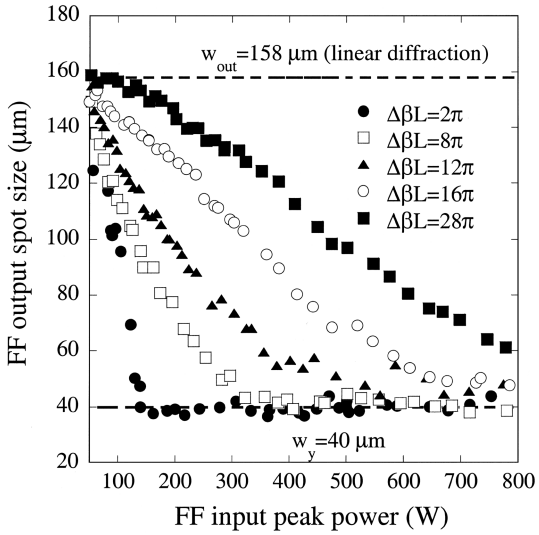

Fig. 3. FF output spot versus FF input power at various values of $\Delta\beta L$. The expected output spot under linear diffraction ($w_{\mathrm{out}} = 158$ μm) and the input value ($w_y = 40$ μm) are also indicated.

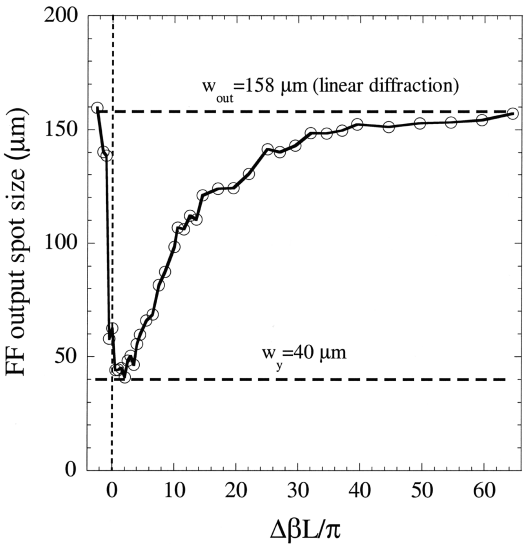

Fig. 4. FF output spot versus $\Delta\beta L$ for a FF input power of 190 W. The vertical dashed line indicates phase matching.

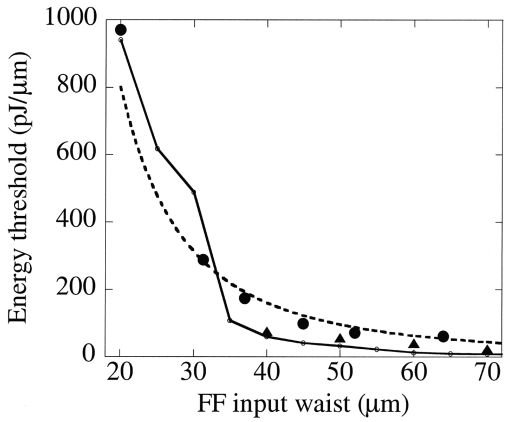

Fig. 5. Measured waist-threshold scaling: experimental values (filled circles and triangles; see text) and energy-law fit $E_{\mathrm{th}} \propto w_y^{-2.3}$ (dashed curve). The solid curve was generated by a cw beam-propagation method and $d_{\mathrm{eff}} = 0.9 d_{\mathrm{eff,\,ideal}}$.

large waists the total sample length only slightly exceeded the diffraction distance, the data trend and the numerical simulations clearly indicate that a quadratic soliton was being excited.

Employing a sample with $L = 2.45$ cm, $\Gamma = 2$ mm, and $\Lambda = 16.25$ μm, we explored self-trapping for smaller FF input waists, as also shown in Fig. 5 (circles). The data were interpolated with $P_{\mathrm{th}} \propto w_y^{-2.3}$ (dashed curve), in good agreement with the literature.[14] Finally, extensive beam propagation method simulations led to $d_{\mathrm{eff}} = 0.9 d_{\mathrm{eff,\,ideal}}$, well compatible with the presence of defects in the poled areas (as observed by direct inspection).

In conclusion, we have investigated one-dimensional simulton generation in reverse-proton-exchanged samples. To the best of our knowledge, the reported powers are the lowest employed to date for the FF excitation of quadratic spatial solitons in uniform-grating (nonchirped) quasi-phase-matched planar waveguides in $LiNbO_3$. The result, stemming from the large overlap integral between FF and SH zeroth-order eigenmodes in buried proton-exchanged RPE waveguides, should allow for even lower thresholds with optimized $\chi^{(2)}$ gratings and longer, low-loss samples. In this respect, we note that propagation losses in channel RPE optical frequency converters have already been reduced to 0.13 dB/cm,[15] and RPE PPLN 1.55-μm doublers with uniform quasi-phase matching for a length of 6 cm have been demonstrated.[16] Such loss and poling characteristics are comparable with those of state-of-the-art Ti indiffused waveguides, and we are confident of achieving similar values in planar RPE waveguides without diminution of the conversion efficiency.

G. Assanto's e-mail address is assanto@ele.uniroma3.it.

References

1. H. Nishihara, M. Haruna, and T. Suhara, *Optical Integrated Circuits* (McGraw-Hill, New York, 1989).
2. Y. N. Korkishko, V. A. Fedorov, T. M. Morozova, F. Caccavale, F. Gonella, and F. Segato, J. Opt. Soc. Am. A **15,** 1838 (1998).
3. J. L. Jackel and J. J. Johnson, Electron. Lett. **27,** 1360 (1991).
4. J. Olivares and J. M. Cabrera, Appl. Phys. Lett. **62,** 2468 (1993).
5. A. Di Lallo, A. Cino, C. Conti, and G. Assanto, Opt. Express **8,** 232 (2001), http://www.opticsexpress.org.
6. A. Amoroso, A. Di Falco, G. Leo, G. Assanto, A. Parisi, A. Cino, and S. Riva Sanseverino, IEEE Photon. Technol. Lett. **15,** 443 (2003).
7. M. Yamada, N. Nada, M. Saitoh, and K. Watanabe, Appl. Phys. Lett. **62,** 435 (1993).
8. K. R. Parameswaran, R. K. Route, J. R. Kurz, R. V. Roussev, M. M. Fejer, and M. Fujimura, Opt. Lett. **27,** 179 (2002).
9. G. Assanto and G. I. Stegeman, Opt. Express **10,** 388 (2002), http://www.opticsexpress.org.
10. R. Schiek, Y. Baek, and G. I. Stegeman, Phys. Rev. E **53,** 1138 (1996).
11. P. Pioger, V. Couderc, L. Lefort, A. Barthelemy, F. Baronio, C. De Angelis, Y. Min, V. Quiring, and W. Sohler, Opt. Lett. **27,** 2182 (2002).
12. G. Leo, L. Colace, A. Amoroso, A. Di Falco, and G. Assanto, Opt. Lett. **28,** 1031 (2003).
13. A. V. Buryak and Y. S. Kivshar, Opt. Lett. **19,** 1612 (1994).
14. L. Torner, in *Beam Shaping and Control with Nonlinear Optics*, F. Kajzar and R. Reinisch, eds., Vol. 369 of NATO ASI Ser. B (Plenum, New York, 1998), p. 229.
15. R. V. Roussev, A. Sridharan, K. Urbanek, R. L. Byer, and M. M. Fejer, in *IEEE-LEOS '03 Annual Meeting* (Institute of Electrical and Electronics Engineers, Piscataway, N.J., 2003), Vol. 1, p. 334.
16. Z. Jiang, D. S. Seo, S.-D. Yang, D. E. Leaird, R. V. Roussev, C. Langrock, M. M. Fejer, and A. W. Weiner, "Low power, high-contrast coded waveform discrimination at 10 GHz via nonlinear processing," IEEE Photon. Technol. Lett. (to be published).